Results in Engineering 31 (2026) 111610

Contents lists available at ScienceDirect

Results in Engineering

journal homepage: www.sciencedirect.com/journal/results-in-engineering

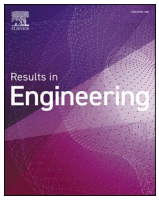

Research paper

# Pressure-induced structuring and yield stress of waxy crude oils

María J. Martín-Alfonso [a,*], Francisco J. Martínez-Boza [a], Pedro Partal [a], F. Javier Navarro [a], Erika M. Sánchez-Ramos [b]

[a] Pro²TecS-Chemical Process and Product Technology Research Centre, Department of Chemical Engineering, ETSI, Campus de "El Carmen", Universidad de Huelva, 21071 Huelva, Spain

[b] Repsol Technology Lab. Repsol SA. Paseo de Extremadura, Km 18, 28935 Móstoles, Madrid, Spain

ARTICLE INFO

*Keywords:*
Crude oil
Yield stress
High-pressure rheology
High-pressure calorimetry
WAT

ABSTRACT

The rheological behavior of waxy crude oils at low temperatures is highly dependent on pressure, temperature, and composition. This study investigates the effects of pressure, pressurization conditions, and aging on the flow behavior and yield stress of three waxy crude oils with different wax contents and WAT values. Differential scanning calorimetry and high-pressure rheometry were performed under controlled thermal and pressure conditions up to 300 bar. Viscosity followed an exponential pressure dependence consistent with Barus law, with piezoviscous coefficients of 18–20 $GPa^{-1}$ at 60 °C and 26–32 $GPa^{-1}$ at 4 °C. Pressure increased the WAT by approximately 0.25 °C $MPa^{-1}$ and promoted earlier gelation. When applied at the onset of cooling, pressure significantly enhanced gel strength, whereas late pressurization reduced yield stress and produced a more gradual yielding process. After 1 h of aging, yield stress increased by approximately 0.3% per bar. The pressurizing medium also affected the gel structure. Using crude oil as the pressure-transmitting fluid produced the highest gel strength, while nitrogen caused minor reductions and helium induced a more pronounced weakening effect. The extended Sisko-Barus model accurately described the flow behavior. These findings demonstrate that pressure history and aging significantly modify gel structure and yield behavior, with important implications for flow assurance in subsea pipeline operations.

## 1. Introduction

Crude oil from deep-water or Arctic wells is often exposed to low temperatures during production and transportation. Under these conditions, when flow stops, the temperature of the crude oil can drop below the wax appearance temperature (WAT). This leads to the initial crystallization of n-paraffin in the liquid phase. This partial liquid-solid transition continues below the pour point, resulting in extensive wax crystal flocculation, which promotes undesirable phenomena such as fluid gelation and deposition. Ultimately, this can lead to pipeline blockage ([1–5]).

The gelation of crude oil at low temperatures is a complex process influenced by several factors [6], including the nature and composition of the crude [7] , thermal and shear histories [1,8], initial cooling temperature [9,10], cooling rate, and pressure [11,12]. The interaction among high-molecular-weight components, such as crystallized n-paraffins, and the presence of resins [13] and asphaltene clusters also influence both wax crystallization and gelation in crude oil [14–17]. In addition, the presence of emulsified water droplets plays a critical role in promoting gelation and nucleation, with smaller droplets and higher water volume fractions increasing nucleation rates [18]. These phenomena induce intricate structural changes within the fluid matrix, significantly affecting the rheological behavior of the crude. Specifically, the fluid transitions from simple Newtonian behavior at temperatures above the WAT to complex non-Newtonian behavior near and below the pour point, develops shear thinning, yield stress, and thixotropic effects [19–22]. This non-Newtonian behavior has profound implications for flow assurance in pipelines, particularly in terms of system sizing, the frequency of remedial operations [23], and the design of restart processes following programmed or accidental shutdown [1, 24–26,4,27,28].

The thermo-rheological complexity of waxy crude oils at low temperatures makes it difficult to determine reliable and reproducible flow properties in these systems [29]. Researchers have undertaken extensive efforts to address this issue by controlling relevant variables during experimentation [30]. These include crude composition, light ends, previous shear and thermal histories, cooling rate, and aging [31–33].

* Corresponding author.
*E-mail address:* mariajose.martin@diq.uhu.es (M.J. Martín-Alfonso).

https://doi.org/10.1016/j.rineng.2026.111610
Received 4 November 2025; Received in revised form 2 June 2026; Accepted 17 June 2026
Available online 18 June 2026
2590-1230/© 2026 The Author(s). Published by Elsevier B.V. This is an open access article under the CC BY license (http://creativecommons.org/licenses/by/4.0/).

*List of Acronyms*

| | |
|---|---|
| *WAT* | Wax appearance temperature (°C) |
| $\eta$ | Viscosity (Pa·s) |
| $\eta_\infty$ | Infinite-shear viscosity in the Sisko model (Pa·s) |
| $n_o$ | Flow index of the Sisko model (-) |
| $k_o$ | Consistency index (Pa·s$^{(Pa)}$) |
| $k_1$ | Fitting parameter describing the pressure dependence of the consistency index (Pa·s$^{(Pa)}$/bar) |
| $n_1$ | Fitting parameter describing the pressure dependence of the flow index (bar$^{-1}$) |
| $\beta_o$ | Barus piezoviscous coefficient at constant temperature (bar$^{-1}$) |
| $\beta_1$ | Fitting parameter describing deviations from the Barus coefficient (bar$^{-2}$) |
| P | Applied pressure (bar) |
| $P_r$ | Reference pressure (bar) |
| $\dot{\gamma}$ | Shear rate (s$^{-1}$) |
| $\tau$ | Shear stress (Pa) |
| $\gamma$ | Deformation (-) |
| $N_2$ | Nitrogen gas |
| *He* | Helium gas |

Yield stress is recognized as a crucial rheological parameter for designing the restart process in gelled pipelines and has received particular attention. Wardhaugh and Boger [34] defined three types of yield stress: elastic at low deformation, followed by a static or true at intermediate deformation, and dynamic at high deformation which is associated with fracture and the onset of flow. From a practical standpoint, the solid-liquid transition occurs once critical stress is exceeded, resulting in observable flow of the material [35]. The value attributed to this critical yield stress/strain depends on the specific definition adopted ([36,24,31,26,37]. Furthermore, flow instabilities such as wall slip can significantly affect the accurate determination of rheological properties such as yield stress due to the complex particulate structure and viscoelastic nature of gelled crude oil. Dimitriou et al. [38] demonstrated that wall slip can markedly alter the bulk flow behavior, underscoring the importance of accounting for this phenomenon in pipeline flow measurements. Marchesini et al. [21] proposed an experimental protocol designed to ensure consistent thermal and shear histories, thereby minimizing variability introduced by wall-slip effects during measurements. More recently, Marinho et al. [39] investigated the impact of wall slip on gelled waxy oils. They concluded that understanding such effects is essential for deriving the accurate rheological properties required for the effective design of transport systems. Various methodologies have been proposed to mitigate wall-slip issues, including the use of vane geometries [40,41] and roughened surfaces [42,39].

The rheological characterization of gelled crude oils is typically carried out under ambient pressure conditions [9,43,44,21]. However, these conditions differ substantially from the high-pressure environments encountered on the seabed. This discrepancy is particularly relevant during shutdowns and the restart of a pipeline obstructed by gelled crude because high-pressure pumping conditions are required to break the gel and reinitiate flow [45]. Recent studies have shown increasing interest in examining the effects of pressure on oil systems [46–48]. Vieira et al. [49] 2223F2investigated the impact of pressure on wax crystallization using differential scanning calorimetry (DSC) and various saturation gases to simulate real flow conditions occurring in pipelines during temperature decreases. Their careful selection of experimental conditions yielded reproducible results, revealing that wax solubility is negatively affected by pressure. Additionally, Li and Gong [50] examined the impact of pressure on waxy crude oil containing water and found that pressure increased WAT values, approximately 0.1 °C/MPa, while water content had a minimal effect on WAT evolution. Similarly, in their study, Li et al. [12] explored the effects of a pressure-responsive additive on wax crystallization and the rheological properties of crude oil under nitrogen pressure. They observed a slight increase in WAT with rising pressure, which was consistent with other previously reported studies [51,49] 25F2. They noted substantial increases in viscosity and yield stress at temperatures well below the WAT/pour point using inert gas ($NR_2R$) to pressurize the samples. Mortazavi-Manesh and Shaw [52] 26F examined the rheological behavior of Maya crude oil under varying pressure conditions and determined that pressure heightened the viscosity and accelerated the reconstruction of the microstructure. In this regard, Sakthivel and Velusamy [53,54] demonstrated that selected ionic liquid additives can mitigate these negative effects. These studies demonstrate that flow operations became more susceptible to the effects of non-Newtonian behavior under pressure. Despite these previous investigations under pressure, there is still a lack of a consistent mechanistic understanding of how pressure alters crystallization thermodynamics, microstructural reconstruction, and yield stress development that motivated this work. In particular, the combined effect of pressure magnitude, pressure history, and pressurizing medium has not been systematically examined under controlled rheological conditions. In this context, the primary objective of this study is to examine the rheological behavior of selected waxy crude oils by evaluating the effects of pressure, pressure history, and pressurizing fluids on the non-Newtonian behavior and yield stress of gelled crude oils at temperatures below the WAT.

The underlying hypothesis of this work is that pressure not only shifts thermodynamic equilibrium conditions, as reflected in the increase of WAT, but also modifies the structural organization and compaction of the wax crystal network during gel formation, thereby controlling the magnitude and pressure-history dependence of the measured yield stress.

This study bridges the lack of systematic understanding of how pressure affects the microstructural development and gel strength of waxy crude oils below the pour point. It also addresses the need to validate experimental protocols that isolate pressure effects from thermal and shear histories under controlled laboratory conditions, as well as the limited quantitative information available on how different pressurizing media influence yield stress and non-Newtonian behavior during gel formation. By tackling these issues, this study aims to provide physically consistent insights into pressure-dependent gelation mechanisms relevant to subsea pipeline operation.

This study presents the novel determination and comparison of yield stress in gelled crude oils under pressure and temperature conditions representative of the seabed, evaluating the effect of pressurizing with different fluids (liquids and gases). These results can contribute to the development of predictive models that can extrapolate laboratory measurements to subsea environments (high pressure and low temperature), which can help with the engineering design of pipeline restart operations.

## 2. Materials and methods

### 2.1. Materials

Three dead crude oil samples, designated as Sample S, Sample L, and Sample M, were provided by Repsol S.A. The physical properties of the crude oil samples, including API gravity, wax appearance temperature (WAT), and SARA fractions, are presented in Table 1.

### 2.2. Methods

#### 2.2.1. Differential scanning calorimetry (DSC)

Calorimetric analyses were conducted using two calorimeters. Experiments at ambient pressure were carried out with a modulated T-zero calorimeter TA Instruments Q100 (USA). Samples of about 10–15 mg, enclosed in hermetic aluminum pans, were subjected to a cooling

**Table 1**
Physical characteristics of the crude oil samples.

| Crude Sample | API Gravity | Density at 15 °C (g/mL) | Density at 40 °C (g/mL) | Dynamic viscosity at 60 °C (mPa·s) | WAT (°C) | Pour Point (°C) | Wax content[a] (wt %) | Saturates (wt%) | Aromatics (wt%) | Resins (wt%) | Asphaltenes (wt%) |
|---|---|---|---|---|---|---|---|---|---|---|---|
| Crude S | 29.0 | 0.8823 | 0.8635 | 8.5 | 26.88 | 6 | 8.27 | 53 | 12 | 34 | 1 |
| Crude L | 22.7 | 0.9183 | 0.8823 | 34.4 | 50.5 | 12 | 5.02 | 48 | 15 | 31 | 5 |
| Crude M | 28.2 | 0.8866 | 0.8656 | 7.7 | 36.51 | 9 | 4.49 | 53 | 9 | 35 | 3 |

[a]Values obtained from DSC at 5 °C/min.

temperature program from 80 °C to −50 °C, at the rate of 5 °C/min.

High-pressure calorimetry was performed using a Calvet SETARAM 3D C80 micro-calorimeter equipped with high-pressure stainless-steel cells of 2.5 mL capacity. This device accommodates a significantly larger sample volume than conventional T-zero calorimeters (up to 2500 mg), which, when combined with the high sensitivity of the 3D sensor, enables the detection of subtle thermodynamic transitions. The measurement protocol consisted of the following three consecutive steps: (1) linear heating from room temperature up to 80 °C at a rate of 1 °C/min, (2) isothermal equilibration at 80 °C for 1.5 h, (3) cooling down to a temperature of 30 °C (the lower temperature limit of this device), at a rate of 10 °C/h (0.1667 °C/min). Samples were pressurized either with the crude oil itself or with inert gases ($N_2$ and He) to a pressure of 300 bar, using an automatic Teledyne-Isco pump (model 260D, USA).

### 2.2.2. *Rheological characterization*

The rheological characterization of the crude oils was conducted in a Controlled-Stress Rheometer (Haake Mars II, Germany), which was equipped with various geometries and a coaxial cylinder pressure cell. Atmospheric pressure rheological data were obtained using several standard coaxial cylinder geometries (inner diameters of 27 mm and 41 mm, respectively, and a gap of 1 mm). In addition, rough surface plate-plate and coaxial cylinder geometries were used to minimize the influence of wall slip. Pressurized rheological data were obtained at 300 bar using a non-conventional coaxial cylinder pressure cell (D400/300), equipped with an inner cylinder of 37 mm diameter and a 1 mm gap (PZ37R). Both the pressure cell and the inner cylinder were mechanically modified to provide roughened surfaces. The cell was magnetically coupled to the rheometer. A DC5 circulating water bath (Haake) was used to control the temperature (with a precision of ±0.1 °C) during cooling, aging, and rheological measurements.

### 2.2.3. *Temperature and pressure cooling protocol*

The preparation of waxy crude oil samples for rheological characterization consisted of three main steps, as described by Marchesini et al. [21]. First, the entire sample was homogenized at 80 °C in a closed container for 30 min with intermittent agitation and storage at 60 °C. In the second step, the sample was placed on the rheometer and cooled to the measurement temperature while at rest, with a cooling rate of 10 °C/h (0.166 °C/min). In the third step, the sample was aged at rest for one hour before the rheological test. Additionally, the ageing period was extended to 8 h for selected samples. Each test was performed in duplicate, with a relative standard deviation of 5% or less between replicates.

The waxy crude oil samples were pressurized using an automatic Teledyne Isco pump (model 260D) according to the experimental configuration shown in Fig. 1. The crude oil was poured into the D400/300 pressure cell at 60 °C. The cell was then sealed and mounted on the rheometer's cooling/heating system. The sample was pressurized with either liquid crude oil or inert gas at ambient temperature to transmit pressure. A sample cylinder was used to separate the pressurizing fluid from the test crude oil and to prevent direct contact between the two. In a separate set of experiments, inert gases ($N_2$ and He) were used directly as pressurizing fluids, allowing contact with the crude oil sample.

In every experiment, the pressure cell was filled by pumping fresh crude oil from the sample cylinder at 60 °C. The operating sequence depends on the pressurizing medium used.

**(A) Crude oil as pressurizing fluid**

1. The pressure cell was filled by opening valves 2, 3, 7, and 8, while valves 4, 5, and 6 remained closed.
2. Air was removed prior to filling either by applying a vacuum (≈1 mbar) through valve 5 or by inverting the cell and venting through valves 4 and 5 while valve 3 was closed.
3. Once filled and sealed, pressure was applied by the Isco pump to the sample cylinder. The floating piston transmitted pressure to the test crude oil without direct mixing between the pressurizing fluid and the sample.
4. The desired pressure was then maintained during the cooling and aging stages.

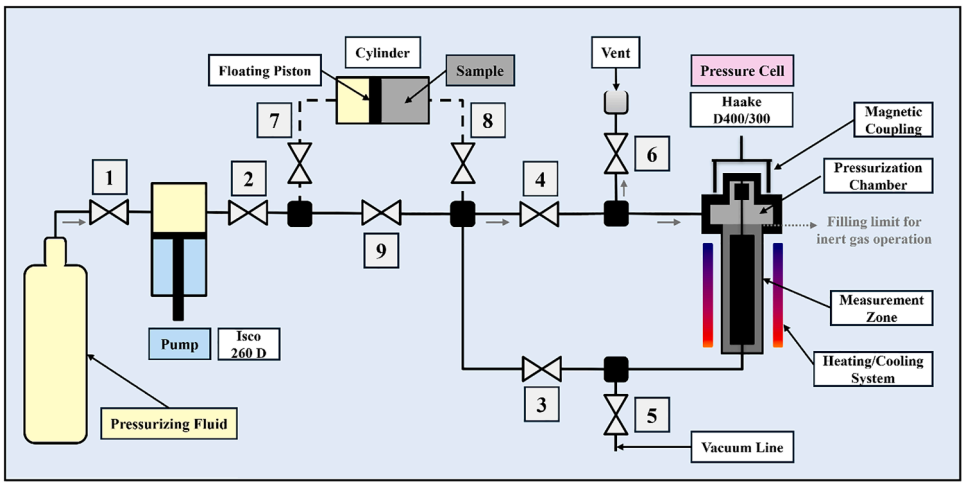


**Fig. 1.** Schematic diagram of the experimental setup developed for yield stress measurements under pressure (control valves are indicated as 1–9).

**(B) Inert gas as pressurizing fluid in direct contact with crude oil ($N_2$ or He)**

1. The pressure cell was first filled with crude oil, up to the measurement zone (slightly above the inner coaxial-cylinder height; gray region in Fig. 1).
2. Valves 6, 7, 8, and 3 were closed to isolate the sample.
3. Valves 9 and 4 were opened to allow the inert gas to pressurize the crude oil directly.
4. The gas remained in contact with the crude oil throughout the cooling, aging, and rheological testing stages.

In all configurations, the Isco pump supplied and regulated the pressure via valves 2 and 4, ensuring stable pressure control during the entire pressure–temperature program.

## 3. Results and discussion

### 3.1. Rheological and thermal behavior of crude oil under pressure

It is well known that crude oils behave like Newtonian liquids at temperatures above the wax appearance temperature (WAT). Well above the WAT, paraffins remain in the liquid state, and viscosity becomes independent of both thermal and shear histories. From a rheological perspective, the crude behaves as a simple fluid characterized by a constant viscosity at a given temperature (see Table 1). The effect of pressure on rheology in the liquid regime is an increase in viscosity, as has been pointed out elsewhere [50,55]. In this range of pressure, viscosity follows an exponential trend that can be described by a piezoviscous or pressure coefficient. The values of the piezoviscous coefficient at 60 °C were calculated using the exponential Barus' law between ambient pressure and 300 bar, yielding values of 18.6, 20.0, and 18.7 $GPa^{-1}$ for crudes S, L, and M, respectively. These values are typical for hydrocarbons in the liquid regime [55–57].

In contrast, below the WAT, the rheological behavior of waxy crude oil is strongly dependent on the thermal and shear histories, particularly within the temperature range in which paraffin crystallization occurs and the subsequent fluid gelation [21,8]. This region can be determined using several techniques, including viscometry, microscopy, and differential scanning calorimetry (DSC) [58,11]. In this study, Fig. 2 shows the thermograms as cooling curves obtained from conventional DSC. The onset of the first endothermic peak (Fig. 2A) has been characterized as the WAT, according to Kok et al. [59,60]. The corresponding values for the samples studied are presented in Table 1. Crude oil S exhibits the lowest WAT, approximately 26 °C, and the highest wax content at 8%. Crude oils L and M show similar wax contents of around 5 wt%, but markedly different WAT values. Crude oil L presents the highest WAT, at approximately 50 °C, as can be observed in Fig. 2A, whereas crude oil M shows an intermediate value of 36.5 °C. One possible explanation for this is that the n-paraffins in crude L have longer chains, resulting in structures with higher melting points. In addition, the high asphaltene content can provide surfaces for wax crystals to adhere to, leading to aggregation and promoting the higher melting point [61,15].

The effect of pressure on the DSC cooling curves is presented in Fig. 2B For crude L, the WAT determined at lower cooling temperatures was slightly shifted to higher temperature values (53.7 °C). Pressure increased the WAT up to 61.4 °C at 300 bar, corresponding to an increase of 0.25 °C/MPa. This value is slightly higher than that reported for the increase of WAT with pressure determined by rheological measurements but of the same order as the change in melting point reported for n-paraffins under pressure [12]. This effect has been attributed to the development of a more compact crystalline structure under pressure by high-molecular-weight paraffins [31,62]. In this regard, the background effect of pressure on the Calvet calorimeter was analyzed by measuring the onset of indium crystallization at the same cooling rate. This resulted in an increase of 0.045 °C/MPa between ambient pressure and 500 bar. This indicates good stability in measuring phase transitions under pressure with this device. For samples S and M, the WAT displacement with pressure occurred near the lower temperature limit of the Calvet calorimeter, and it was not possible to determine it accurately under these experimental conditions.

At temperatures below the WAT [63]27F, waxes and high molecular weight components crystallize [60], as can be deduced from the exothermic event shown in the cooling curves of Fig. 2. Crystallization leads to a progressive liquid-solid transition associated with the onset of non-Newtonian behavior, as shown in Fig. 3, where the flow curves at 4 °C, well below the WAT, are displayed. The liquid-solid transition is more apparent at lower temperatures in samples exhibiting higher WAT and greater wax content, as has been pointed out elsewhere [31,61,64].

The gelled structure, resulting from the presence of interconnected

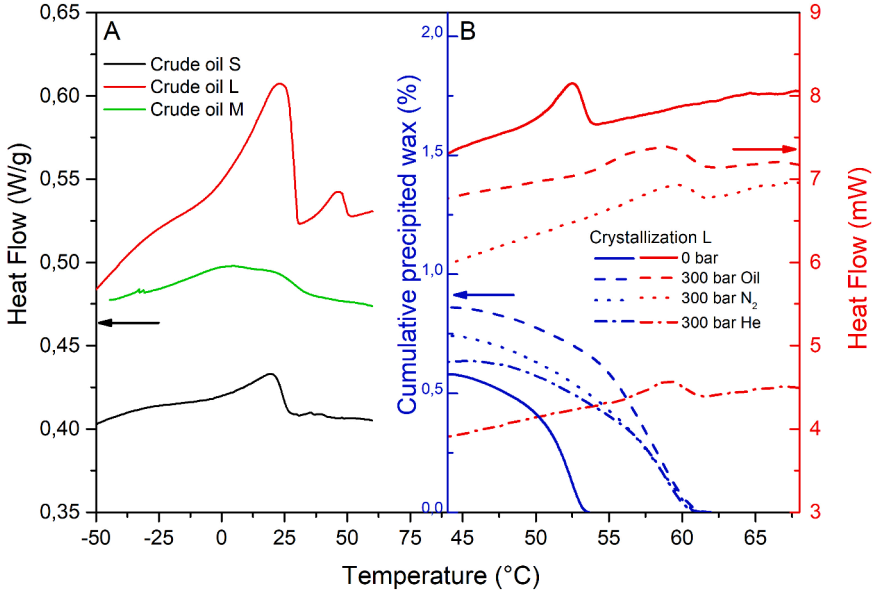


**Fig. 2.** DSC cooling curves for the crude oil samples tested. (A) Cooling thermograms obtained from conventional T-zero DSC at a cooling rate of 5 °C/min for samples S, L, and M. (B) Cooling thermograms obtained from Calvet DSC at 0.1667 °C/min (10 °C/h) for sample L.

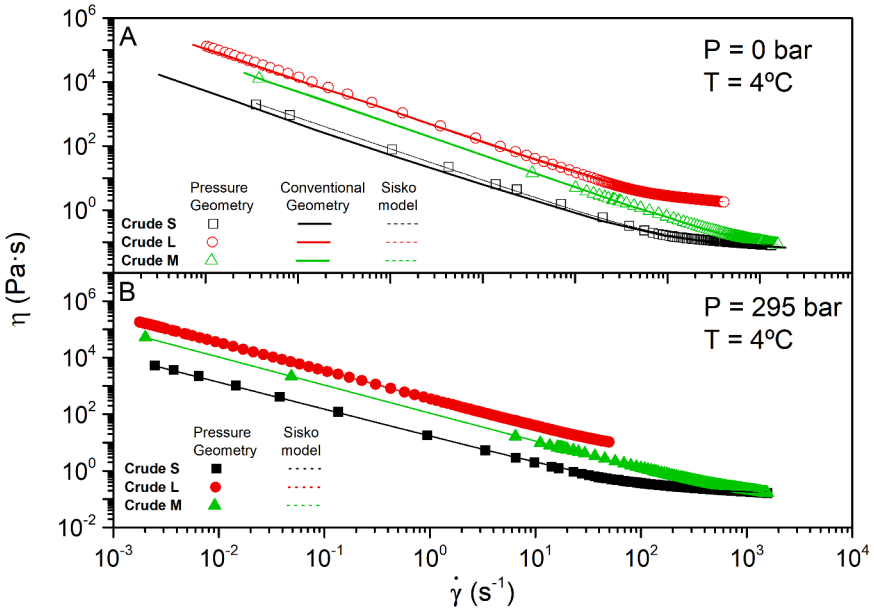


**Fig. 3.** Evolution of viscosity as a function of shear rate for the crude oil samples measured at atmospheric pressure (A) and at 295 bar (B) using pressurized geometry. Viscosity measured using the conventional coaxial-cylinder geometry at atmospheric pressure (solid lines) is included for reference.

soft solid phases, gives rise to complex rheological behavior such as time dependence and pseudoplasticity, including the appearance of yield stress [65]. When this structure is disrupted by an applied stress above the yield stress value, a significant decrease in viscosity is observed, accompanied by a high degree of pseudoplasticity. This behavior can be modeled by a power law at low and intermediate shear rates, with a tendency to reach a limiting viscosity value at higher shear rates, as described by the Sisko model [66]. The Sisko model can be generalized to include the effect of pressure on the flow behavior at constant temperature, resulting in the Sisko-Barus model [48], which has been applied to oil-based drilling fluids [67,68].

$$\eta = \left(\eta_\infty + (k_0 + k_1(P-P_r))\cdot\dot{\gamma}^{(n_0+n_1(P-P_r))-1}\right)\exp\left(\beta_o(P-P_r)+\beta_1(P-P_r)^2\right) \quad (1)$$

where $k_1$ and $n_1$ are fitting parameters that evaluate the impact of pressure on the consistency and flow indexes of the classical Sisko equation. $\beta_o$ is Barus's piezoviscous coefficient at constant temperature, and $\beta_1$ is a fitting parameter that accounts for deviations of Barus's piezoviscous coefficient at higher pressures. P and $P_r$ are the applied and reference pressures, respectively. In this approach, the effect of pressure is quantified mainly by its contribution to the bulk viscosity of the system, represented by the classical Barus pressure coefficient ($\beta_o$), together with a linear estimation of possible deviations from this dependence in the consistency and flow indexes, and in the piezoviscous coefficient, that may occur at higher pressures [68]. The values of the parameters of the Sisko model are shown in Table 2.

At this temperature, pressure mainly causes a marked exponential increase in viscosity values at a given shear rate. Nevertheless, pressure does not substantially modify the values of the consistency and flow indexes of the crude oils tested. Consequently, the parameters $k_1$, $n_1$.and $\beta_1$ have very low values in this pressure-temperature range and can be set to zero without significantly decreasing the precision of the model. The piezoviscous coefficients at 4 °C, calculated using the exponential model between 0 and 295 bar, are higher than those obtained above the WAT, with values of 25.9, 32.0, and 24.4 $GPa^{-1}$ for samples S, L, and M, respectively. The observed increase in the piezoviscous coefficient at low temperatures has been previously reported by several authors [12,56]. The gelled structure that forms at lower temperatures consists of interconnected wax crystals that trap solvent oil and components that have not crystallized [1,31]. This high degree of association increases molecular friction under flow due to the greater density of these compact structures at low temperatures.

### 3.2. Determination of yield stress in the pressure cell

The determination of yield stress in waxy crude oil is a complex task due to the intricate nature of these materials. The solid-liquid transition occurs beyond critical stress that results in observable flow of the material [31]. The value attributed to this critical yield stress depends on the specific definition of critical stress and the criteria adopted for considering that the material is flowing. In addition, the use of pressurized geometries may introduce additional sources of error that can be quantified by comparing the results obtained from conventional and non-conventional geometries. In this regard, Fig. 4 compares the viscosity curves versus shear stress measured using both conventional coaxial cylinders and pressurized coaxial cylinders for the crude oils studied at atmospheric pressure.

As can be observed (Fig. 4), for crude oils S and M a sudden drop in the viscosity curves versus shear stress is observed, with yield-stress values of 65.6 ± 5 Pa and 268.5 ± 7 Pa, respectively. This indicates a sharp breakdown of the gelled structure, which is the main characteristic of the solid-liquid transition for these samples and permits the

**Table 2**
Parameters of the extended Sisko-Barus model for the crude oils studied at 4 °C.

| | $k_o$ (Pa·s$^{(n_o)}$) | $k_1$ (Pa·s$^{(n_o)}$/bar) | $n_o$ | $n_1$ (bar$^{-1}$) | $\eta_\infty$ (Pa·s) | $\beta_o$ (bar$^{-1}$) | $\beta_1$ (bar$^{-2}$) | $R^2$ |
|---|---|---|---|---|---|---|---|---|
| Crude S | 8.18±0.07 | 0 | 0.0407±0.002 | 0 | $0.0744\pm3\cdot10^{-4}$ | $0.00259\pm1\cdot10^{-5}$ | 0 | 0.989 |
| Crude L | 129.6 ± 0.5 | 0 | 0.010±0.001 | 0 | $1.491\pm3\cdot10^{-3}$ | $0.0032\pm1\cdot10^{-5}$ | 0 | 0.995 |
| Crude M | 53.0 ± 0.2 | 0 | 0.012±0.001 | 0 | $0.0472\pm3\cdot10^{-4}$ | $0.00244\pm7\cdot10^{-6}$ | 0 | 0.998 |

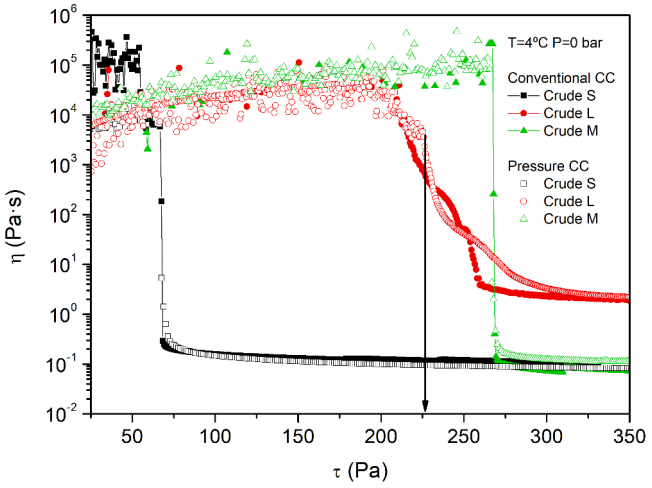


**Fig. 4.** Viscosity curves versus shear rate for the crude oils samples S, L and M, at atmospheric pressure and the temperature of 4 °C.

unambiguous determination of a critical yield stress value, independently of the device used, conventional or pressure cell. Nevertheless, for crude oil L, the yielding process is more complex: the initial solid-like state degrades into a liquid-like state through an intermediate viscoelastic region, characterized by a stepwise drop in viscosity as shear stress increases. The multi-stage yielding process suggests the presence of a heterogeneous gel formed by several phases of different strength [26,37]. This interpretation is supported by the occurrence of multiple crystallization events in the DSC thermograms (see Fig. 2A). These events likely reflect the solidification of different paraffinic fractions over a range of temperatures, leading to the formation of crystalline domains with varying structural organization and mechanical strength. As a result, the gel network of crude oil L may exhibit spatial heterogeneity, with regions of different rigidity and connectivity. Under increasing shear stress, these domains are expected to undergo progressive structural breakdown rather than a single catastrophic failure, consistent with the observed stepwise decrease in viscosity and the extended viscoelastic region [16]. This structural heterogeneity provides a plausible explanation for the multi-stage yielding behavior and the difficulty in defining a single, well-defined yield stress value for this sample, as heterogeneous solid-liquid transitions have been previously reported in waxy systems [5].

However, a representative yield stress value of 228.5 ± 18 Pa was measured at the first inflection point of the viscosity-stress curve. The actual viscous-flow region extends beyond this value up to approximately 260 Pa. Pressurized geometries introduce additional instabilities in the viscosity-stress curve shape for the highly viscous crude oil sample. For crude oils S and M, which have lower viscosities at 60 °C and 4 °C (see Table 1 and Fig. 3, respectively), the influence of the lower sapphire bearing of the pressure geometry on viscosity can be considered negligible. However, for crude oil L, the yielding process extends over a wide range of shear stress when the sample is tested using the pressure geometry, near 285 Pa. Nevertheless, from a practical point of view, significant flow of the sample occurred at higher stress values due to the influence of the viscous background at this temperature [69]. Additionally, it has been reported that roughened cylinder geometries do not entirely prevent wall slip. This may compromise the quantitative accuracy of yield stress determination, thereby minimizing its value [40,39]. However, in this study, the contribution of wall slip is assumed to be minimal compared to other experimental limitations, such as the presence of sapphire bearings in contact with the gelled oil.

### 3.3. Influence of pressure on the yielding process

The influence of pressure on the gelation of waxy crude oils and its subsequent effect on the yielding process is a matter of considerable importance in the context of pipeline restart operations in subsea environments [34]. In deepwater oilfields, crude oil may cool and gel after shutdown under static conditions. These conditions are characterized by low temperatures and high hydrostatic pressures that increase with depth (e.g. approximately 4 °C and 300 bar at a depth of around 3000 m). To study the influence of the pressure history on the yielding behavior of crude oil, pressure was applied at various stages of the cooling process, as outlined in the experimental section (2.2.3). As a standard procedure, a pressure of 300 bar was progressively applied to a crude oil sample in the liquid state at 60 °C, using the crude itself as the pressure-transmitting fluid. This pressure was maintained throughout the gelation process until the yield stress was measured, as described in Fig. 5A.

As shown in Fig. 5B, where crude oil S is presented as an example, pressure significantly influences both the yielding process and the magnitude of the yield stress. When pressure is applied at the beginning of the cooling process, at 60 °C, and maintained throughout the gel formation process, the yield stress increases from 65.6 ± 5 Pa to 152.4 ± 6 Pa. Moreover, a comparison of the stress-strain curves at 0 and 300 bar shows that the transition from solid-like to liquid-like behavior is very similar at both pressures, except for the value of the yield stress measured. Previous studies, and the DSC results obtained in this work, show that the gelation temperature increases with pressure. Therefore, pressure induced structuring occurs earlier, and gel strength is enhanced, leading to higher yield stress values [45,50,12,52,56,49]. In addition, DSC results (Fig. 2) indicate an increase in the extent of crystallization under pressure within the experimentally accessible temperature range. Since crystallization begins at higher temperatures under pressure, the temperature interval available for crystal growth before reaching 4 °C is extended. This modification of the crystallization window may contribute to the development of a mechanically stronger gel network during cooling under pressure. Consequently, the higher solid fraction and enhanced crystal-crystal interactions within the compacted matrix may partly explain the increase in yield stress values observed at 300 bar.

A negative influence on the yielding process is observed when pressure is applied at the end of the cooling ramp, just at the start of the aging process. These conditions are less representative of real field scenarios; however, they can shed light on how pressure affects the mechanical behavior of the gelled structure. In this case, the yield stress decreases to 52.8 ± 6 Pa, which is lower than the value recorded at atmospheric pressure (65.6 Pa). Moreover, the transition from solid-like to liquid-like behavior is not gradual, and a shoulder appears in the stress-strain curve at intermediate deformations, increasing the uncertainty in determining the yield stress value accurately. Furthermore, when pressure is applied at the end of the aging period, immediately before the rheological test (i.e. no aging under pressure), the yield stress decreases even further to 33.7 ± 6 Pa, making it even more difficult to determine the yield stress value accurately. Regardless of the yield stress magnitude, which clearly depends on pressure kinetics, all samples exhibit similar dynamic yield stress following fracture.

These results may be explained by hypothesizing the formation of different internal structures during the cooling process under pressure. These structures are likely to produce distinct fractured behaviors depending on when, and for how long, the sample was pressurized. It is well established that the structure of waxy gels consists of an arrangement of wax crystals of varying sizes [70]. Hydraulic pressure applied during cooling is expected to result in more compact gelled structures with reduced void content compared with those formed at atmospheric pressure [56,49]. Consequently, these denser structures would exhibit higher yield stress values due to the increased degree of interaction between wax crystals within a compacted solid-like matrix. In this

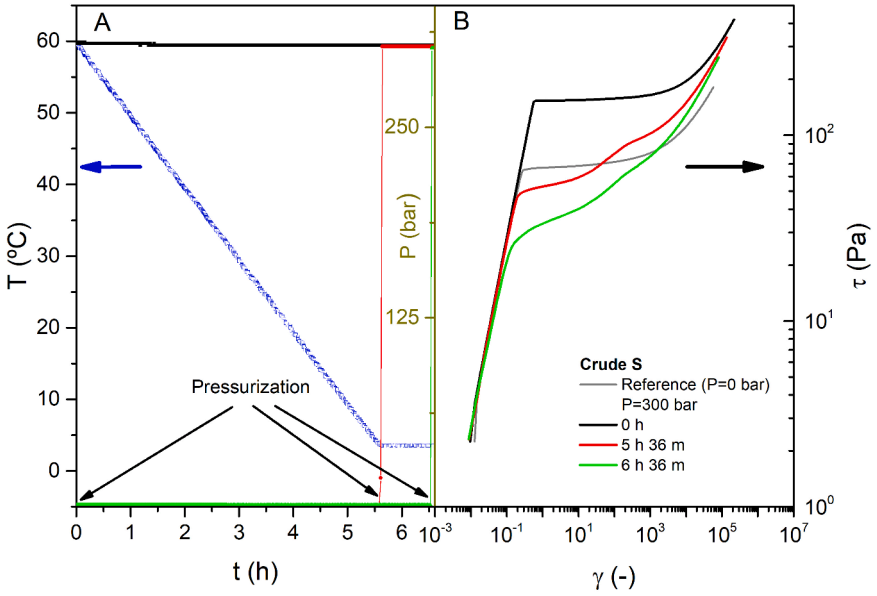


**Fig. 5.** Influence of pressurization on the yield stress. (A) Pressure-temperature-time protocols (pressure applied at the start of the cooling process and after 1 h of gel aging). (B) Stress–strain curves (pressure applied at the start (black), at the end (red), and after aging (green); the reference at zero manometric pressure is included as a thin black line).

context, the sharper fracture transitions observed in Fig. 5B, at both atmospheric pressure and 300 bar, can be attributed to the cohesive failure of a well-interconnected structure composed of large wax crystals that developed during the cooling and aging stages. This behavior is consistent with the dominant mechanism proposed for this cooling rate (10 °C/h) [65], with stronger interconnection forces occurring under pressurized cooling conditions.

In contrast, the gel structure formed under atmospheric pressure during static cooling conditions can develop a significant number of voids that are not uniformly distributed throughout the flocculated wax structure [70]. When pressure is applied immediately prior to the stress ramp, the gel undergoes a reduction in void content due to compression. This compression disrupts and fractures the flocculated network of physical linkages formed by wax crystallization during the cooling process, resulting in a partially weaker and less connected wax structure that exhibits reduced cohesive strength. Upon stress application, the gel exhibits a progressive loss of cohesiveness, characterized by a marked reduction in yield stress values and a non-uniform breakdown of the solid-liquid transition.

An intermediate situation occurs when pressure is applied at the beginning of the aging period. In this case, pressure also disrupts the gelled structure formed at atmospheric pressure during cooling. Probably, the compaction under pressure described above partially breaks the flocculated mesoscale structure of the wax crystals, weakening the interactions among flocs, reducing the cohesive forces, and lowering the overall strength of the bulk structure. However, during the subsequent aging period of one hour, partial anisotropic reorganization and interconnection of wax crystals may occur, leading to a partial recovery of the cohesion observed at atmospheric pressure. This partial recovery results in higher yield stress values and a stepped cohesive failure of the

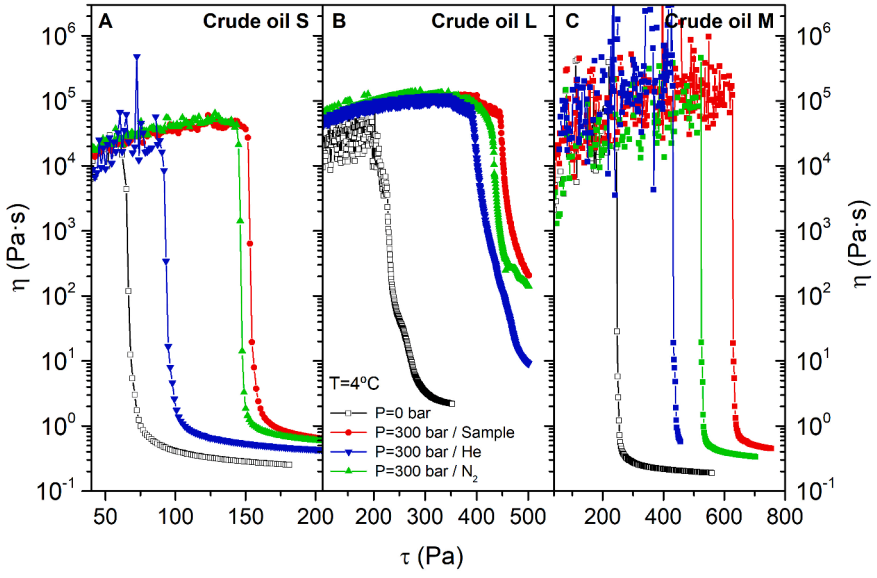


**Fig. 6.** Effect of pressure and pressurization fluid on the yielding behavior of the crude oil samples, obtained from controlled stress tests at 4 °C. (A) Crude oil S. (B) Crude oil L. (C) Crude oil M.

multiphase system. These results show that pressure history could play an important role in the gel strength of waxy crude oils and should therefore be considered when calculating restart pressure [7].

### 3.4. Influence of the pressurization fluid

The pressurizing fluid may also influence the fracture behavior and, consequently, the measured yield stress value, particularly if it is in direct contact with the crude oil. In this context, Fig. 6 presents the viscosity versus shear stress curves for crude oils S, L, and M, obtained under pressure with different fluids.

In all cases, the gel was formed following the cooling protocol shown in Fig. 5A, where a pressure of 300 bar was applied at the beginning of the cooling process (at 60 °C) and maintained constant until the end (at 4 °C), including an aging period of 60 min. The experimental setup was adapted according to the characteristics of the pressurizing fluid. When pressure was applied using the crude oil itself as the pressurizing medium (see Fig. 1), the entire measuring cell was filled with the crude oil sample, including the inner magnetic coupling, upper sapphire bearing, measuring cylinder, and lower sapphire bearing. Pressure was applied automatically from the top by the Isco pump (valve 4 open) and maintained at 300 bar throughout the cooling and gelation processes. These conditions represent a more realistic simulation of field operations in subsea pipelines [24]. Nevertheless, crude oil typically contains dissolved light hydrocarbon gases, which can influence wax crystallization and often improve flowability by reducing WAT, pour point, and yield stress [71,11,72,73]. In contrast, the present study was conducted using degassed crude oil samples to isolate the intrinsic effects of pressure and pressure history on gel formation. Therefore, the rheological parameters obtained here should be interpreted as representative of a conservative scenario in which gas-dissolution effects are minimized. Caution should be exercised when extrapolating these quantitative values directly to live-oil field conditions.

As shown in Figu. 6A and C, a clear gel breakdown is observed for crude oils S and M, with yield stress values of 152.4 ± 6 Pa and 667.4 ± 22 Pa, respectively. However, crude oil L (Fig. 6B) exhibits a more complex transition under these experimental conditions, characterized by an initial elastic region, followed by an extended creep region in which viscosity progressively decreases as shear stress increases, and finally a dynamic yield stress beyond the experimental window. For this sample, it is more difficult to determine a precise critical yield stress, as less clear solid-liquid transition is observed. The value of 448.2± 27 Pa was taken as the yield stress. Nevertheless, at this stress value the sample shows a high viscosity (~$10^4$ Pa·s), as can be seen in the viscosity-stress curve. Consequently, greater stress must be applied to achieve a practically appreciable flow of the sample. These waxy crude oils present flowability issues due to wax crystallization, particularly at high pressures [56]. At 300 bar of crude pressure, the yield stress increases by 132%, 90%, and 148% for crude oils S, L, and M, respectively. The combination of pressure and aging time promotes the development of a denser structure, increasing not only the viscosity values, but also the WAT and the non-Newtonian behavior of the gelled crude, which increases resistance to flow initiation, leading to higher yield stress values compared to atmospheric pressure at the same temperature.

To analyze the effect of pressurizing fluids on yield stress, two inert gases ($N_2$ and He) were used as pressure media, following the experimental setup outlined in Fig. 1. In these experiments, the crude oil sample covered only the lower sapphire bearing and the measuring coaxial cylinder. The magnetic coupling and upper sapphire bearing were filled with the pressurizing gas at a pressure of 300 bar. For this configuration, the pressurized gas remained in contact with the crude oil sample throughout both the gelation and measurement processes and could diffuse into the crude oil, altering the gelled structure and its properties [74,11,12]. As shown in Fig. 6, slightly lower yield stress values were measured when the samples were pressurized with $N_2$ (145.1 ± 5 Pa, 433.5 ± 23 Pa, and 557.6 ± 15 Pa for crude oils S, L, and M, respectively). Consequently, a smaller percentage increase in yield stress was observed under inert gas pressure compared to crude oil pressure (122%, 90%, and 107%, respectively). Furthermore, pressurization with He also increased the yield stress values with pressure (approximately 40%, 73%, and 71% for crude oils S, L, and M, respectively) but resulted in a significant reduction in the yield stress values (92.1 ± 7 Pa, 405.8 ± 23 Pa, and 460.4 ± 16 Pa for S, L, and M, respectively) compared with pressurization with crude oil.

These data support that pressurization with gases alters the cohesiveness of the gelled waxy structure formed under gas pressure during the cooling process, as has been previously reported for both model systems [75] and live crude oils [12,76]. The presence of gases in crude oil may act both as a solvent for paraffins and as a lubricant for high-molecular-weight hydrocarbons. These phenomena may reduce the cohesion among wax crystals and their adhesion at the surface, thereby weakening gel strength and resistance to flow, and consequently reducing the minimum stress required to break the structure and initiate flow. Under the experimental conditions studied, the use of inert gases as pressurizing fluids appears to have little effect on the fracture pattern of the tested crude oils, suggesting low gas diffusion kinetics compared with light hydrocarbon gases [77,73]. The accumulation of significant gas concentrations at the geometry/crude interface, together with the formation of microcavities that could partially reduce surface adhesion and modify the balance between adhesive and cohesive forces, does not appear to dominate the reduction in bulk cohesion associated with the lubricating effect of inert gases. Nevertheless, this assumption has not been experimentally corroborated. As shown in Fig. 6, the solid-liquid transition curves are similar for crude-oil and inert-gas pressurization. The presence of inert gases does not significantly alter the breakdown mechanism but does significantly influence the stress required to initiate flow. This indicates that the yielding process is primarily governed by a reduction in microscopic interactions between wax crystals, probably due to the lower amount of precipitated wax in the presence of inert gases, as reflected by the cumulative precipitated wax values shown in Fig. 2.

On the one hand, the differences in yield stress values for samples pressurized with $N_2$ can be considered within the expected range of experimental uncertainty, supporting the idea that $N_2$ is a suitable pressurizing fluid for conducting tests under pressure with minimal interference in the rheological properties of the sample [10,49]. Conversely, although He has been reported to exhibit lower solubility than $N_2$ in hydrocarbon systems [74], the reduction in yield stress observed under He pressurization may be associated with differences in gas–crude interactions under pressure. Fig. 2 shows that He resulted in the lowest cumulative precipitated wax fraction. Its smaller molecular size likely facilitates permeation through the network, reducing the degree of interconnectivity among wax crystals and resulting in lower cohesive energy than in the case of $N_2$. This behavior is consistent with a more effective lubricating action than that of $N_2$, thereby decreasing the mechanical resistance of the gel network [78]. This interpretation is based on thermodynamic considerations, as the molecular mechanisms underlying this behavior were not directly investigated in the present study.

Finally, the effect of aging time on crude oils S and L was analyzed. Fig. 7 shows shear-stress curves versus deformation at 4 °C and 300 bar of crude oil pressure for aging times of 1 and 8 h. As pointed out in previous studies [31,75], longer aging times increase the yield stress value at atmospheric pressure, but this effect appears to depend on the nature of the crude oil. Crude oil S was more sensitive than crude oil M to aging at atmospheric pressure, with its yield stress increasing by 90% (125 Pa) from 1 to 8 h, compared with an increase of 35% (363 Pa) for crude oil M over the same period.

The effect of pressure for longer aging times (8 h) is slightly less significant than that for 1 h. Taking as reference the value measured at atmospheric pressure after 8 h, the increase in yield stress was 100% (250 Pa) and 93% (703 Pa) for crude oils S and M, respectively. These

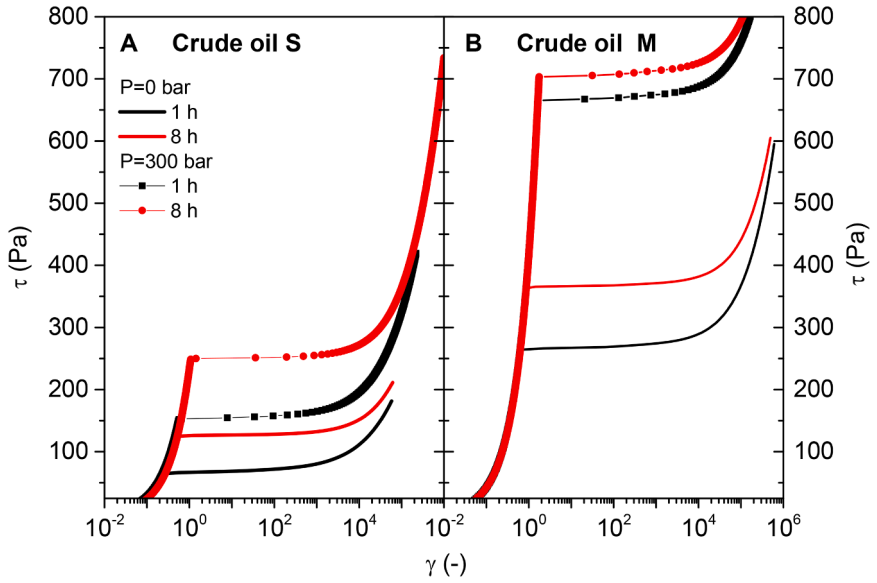


**Fig. 7.** Effect of aging time and pressure on the yielding behavior of the waxy crude oils studied at 4 °C. (A) Crude oil S. (B) Crude oil M.

relative values are slightly lower than those obtained after 1 h of aging at 300 bar (132% and 148%, respectively). Nevertheless, the combined effect of pressure and time (8 h - 300 bar) increases the yield stress by 284% and 162%, respectively, compared with 1 h - 1 bar.

These results indicate that the properties of crude oil drastically affect the waxy structure and its resistance to flow. For crude oil S, the low viscosity facilitates the mobility of wax crystals during cooling and promotes the formation of highly ordered structures with a higher degree of interaction between crystals, leading to increased gel strength [79,8]. A longer aging period enhances the capacity for molecular accommodation within a more interconnected structure, which requires higher stress values to break and initiate flow [44,62,75]. In contrast, for crude oil M, which has high viscosity and a high WAT, the effect of increasing the aging period is less significant in the structuring process probably due to reduced molecular mobility, leading to lower structural enhancement and a smaller increase in yield stress from 1 to 8 h at atmospheric pressure.

Aging under pressure increases viscosity and the amount of precipitated wax, both of which contribute significantly to structural strength. However, it simultaneously reduces free volume, void content, and crystal mobility, thereby masking the contribution of long-term ordering relative to the effect of free-volume reduction caused by pressure structuring [80]. As expected, the combined effect of prolonged aging and pressure is more significant for crude oil S, which has lower viscosity, where the longer time available for ordering and crystal friction leads to higher relative resistance to flow and yield stress.

## 4. Conclusions

Pressure exerts a measurable and systematic influence on the thermo-rheological behavior of waxy crude oils. In the liquid regime above the WAT, viscosity follows an exponential Barus-type dependence on pressure. Below the WAT, the piezoviscous coefficients increase due to gel-network formation and the development of a more structured system. Differential scanning calorimetry confirms that pressure shifts the WAT to higher temperatures (up to ~0.25 °C $MPa^{-1}$ for crude L up to 300 bar), thereby advancing crystallization and promoting earlier gelation.

The yielding response is strongly dependent on pressure history. When 300 bar is applied at the onset of cooling and maintained throughout gelation, yield stress increases significantly (≈0.3% per bar after 1 h aging), while late pressurization weakens the gel and produces more gradual, multi-stage yielding. These findings demonstrate that gel strength is governed not only by pressure magnitude but also by the timing of pressurization relative to crystallization and aging.

The identity of the pressurizing medium further modulates the response. Hydraulic transmission using crude oil produces the highest yield stress values. Nitrogen yields comparable results near experimental uncertainty, indicating minimal rheological perturbation, whereas helium produces a more noticeable reduction in gel strength. Aging enhances gel resistance in a crude-dependent manner: the lower-viscosity crude (S) exhibits greater sensitivity to aging than the more viscous crude (M), and the combined effect of aging under pressure results in the largest strengthening.

From a modeling perspective, the extended Sisko-Barus formulation accurately captures the pressure dependence of the flow curves at 4 °C. Within the explored range, pressure corrections to the Sisko indices ($k_1$, $n_1$) and the quadratic term ($\beta_1$) are negligible, with the exponential Barus contribution dominating the pressure response.

When thermal and pressure histories are rigorously controlled, both pressurization timing and aging duration significantly influence restarting requirements in subsea environments. Nitrogen was found to be less disruptive than helium when direct gas contact is unavoidable. Gas pressurization, particularly with helium, reduces cumulative precipitated wax and gel strength, leading to a weakening of cohesive interactions within the wax crystal network, which may facilitate flow initiation under restart conditions. Limitations include the low-temperature bound of high-pressure calorimetry for certain crudes; future work should expand the temperature window and quantify gas uptake, wax structure, and the diffusion kinetics of inert gases under pressure.

## CRediT authorship contribution statement

**María J. Martín-Alfonso:** Writing – original draft, Visualization, Methodology, Investigation, Formal analysis, Data curation, Conceptualization. **Francisco J. Martínez-Boza:** Writing – review & editing, Visualization, Validation, Supervision, Project administration, Methodology, Investigation, Formal analysis, Data curation, Conceptualization. **Pedro Partal:** Writing – review & editing, Visualization, Funding acquisition, Formal analysis. **F. Javier Navarro:** Visualization, Software, Resources, Funding acquisition, Data curation. **Erika M. Sánchez-Ramos:** Validation, Resources, Project administration, Formal analysis, Conceptualization.

## Declaration of competing interest

The authors declare that they have no known competing financial interests or personal relationships that could have appeared to influence the work reported in this paper.

## Data availability

Data will be made available on request.

## References


[1] G.T. Chala, S.A. Sulaiman, A. Japper-Jaafar, Flow start-up and transportation of waxy crude oil in pipelines-A review, J. Nonnewt. Fluid Mech. 251 (2018) 69–87, https://doi.org/10.1016/j.jnnfm.2017.11.008. Elsevier B.V.

[2] B. Li, Z. Guo, L. Zheng, E. Shi, B. Qi, A comprehensive review of wax deposition in crude oil systems: mechanisms, influencing factors, prediction and inhibition techniques, Fuel 357 (2024) 129676, https://doi.org/10.1016/J.FUEL.2023.129676.

[3] O. Lorge, M. Djabourov, F. Brucy, Crystallisation and gelation of waxy crude oils under flowing conditions, Rev. Inst. Fr. Du Pét. 52 (2) (1997) 235–239, https://doi.org/10.2516/ogst:1997026.

[4] D. Merino-Garcia, S. Correra, Cold flow: a review of a technology to avoid wax deposition, Pet. Sci. Technol. 26 (4) (2008) 446–459, https://doi.org/10.1080/10916460600809741.

[5] R.F.G. Visintin, R. Lapasin, E. Vignati, P. D'Antona, T.P. Lockhart, Rheological behavior and structural interpretation of waxy crude oil gels, Langmuir. 21 (14) (2005) 6240–6249, https://doi.org/10.1021/la050705k.

[6] C. van der Geest, A. Melchuna, L. Bizarre, A.C. Bannwart, V.C.B. Guersoni, Critical review on wax deposition in single-phase flow, Fuel 293 (2021) 120358, https://doi.org/10.1016/j.fuel.2021.120358.

[7] A. Aiyejina, D.P. Chakrabarti, A. Pilgrim, M.K.S. Sastry, Wax formation in oil pipelines: a critical review, Int. J. Multiph. Flow 37 (7) (2011) 671–694, https://doi.org/10.1016/j.ijmultiphaseflow.2011.02.007. Number.

[8] R. Venkatesan, N.R. Nagarajan, K. Paso, Y.B. Yi, A.M. Sastry, H.S. Fogler, The strength of paraffin gels formed under static and flow conditions, Chem. Eng. Sci. 60 (13) (2005) 3587–3598, https://doi.org/10.1016/j.ces.2005.02.045.

[9] D.E.V. Andrade, A.C.B. da Cruz, A.T. Franco, C.O.R Negrão, Influence of the initial cooling temperature on the gelation and yield stress of waxy crude oils, Rheol. Acta 54 (2) (2015) 149–157, https://doi.org/10.1007/s00397-014-0812-0.

[10] H. Li, J. Zhang, C. Song, G. Sun, The influence of the heating temperature on the yield stress and pour point of waxy crude oils, J. Pet. Sci. Eng. 135 (2015) 476–483, https://doi.org/10.1016/j.petrol.2015.10.010.

[11] P. Juyal, T. Cao, A. Yen, R. Venkatesan, Study of live oil wax precipitation with high-pressure micro-differential scanning calorimetry, Energy Fuels. 25 (2) (2011) 568–572, https://doi.org/10.1021/ef101213x.

[12] T. Li, T. Wang, J. Xu, R. Zou, Z. Si, J. Becker, L. Li, M.A. Cohen Stuart, R. K. Prud'Homme, X. Guo, Pressure effect on the rheological behavior of waxy crude oil with comb-type copolymers bearing azobenzene pendant, Ind. Eng. Chem. Res. 57 (14) (2018) 4887–4894, https://doi.org/10.1021/acs.iecr.7b05217.

[13] H. Li, Y. Xie, C. Zhang, H. Li, J. Zhang, Role of resins on wax deposition of waxy oils and its mechanism, Phys. Fluids 37 (2) (2025), https://doi.org/10.1063/5.0253765.

[14] Y. Lei, S. Han, J. Zhang, Effect of the dispersion degree of asphaltene on wax deposition in crude oil under static conditions, Fuel Process. Technol. 146 (2016) 20–28, https://doi.org/10.1016/j.fuproc.2016.02.005.

[15] Y. Lei, H. Wang, S.-S. Li, X.-Q. Liu, H.-R. Zhu, Y.-M. Gao, H.-P. Peng, P.-F. Yu, Effect of existence state of asphaltenes on the asphaltenes-wax interaction in wax deposition, Pet. Sci. 20 (1) (2023) 507–514, https://doi.org/10.1016/j.petsci.2022.08.028.

[16] H. Li, J. Zhang, Q. Xu, C. Hou, Y. Sun, Y. Zhuang, S. Han, C. Wu, Influence of asphaltene on wax deposition: deposition inhibition and sloughing, Fuel 266 (2020) 117047, https://doi.org/10.1016/j.fuel.2020.117047.

[17] H. Xue, J. Zhang, S. Han, M. Sun, X. Yan, H. Li, Effect of asphaltenes on the structure and surface properties of wax crystals in waxy oils, Energy Fuels. 33 (10) (2019) 9570–9584, https://doi.org/10.1021/acs.energyfuels.9b01825.

[18] Z. Wang, Y. Bai, H. Zhang, Y. Liu, Investigation on gelation nucleation kinetics of waxy crude oil emulsions by their thermal behavior, J. Pet. Sci. Eng. 181 (2019) 106230, https://doi.org/10.1016/j.petrol.2019.106230.

[19] M.T. Ghannam, S.W. Hasan, B. Abu-Jdayil, N. Esmail, Rheological properties of heavy & light crude oil mixtures for improving flowability, J. Pet. Sci. Eng. 81 (2012) 122–128, https://doi.org/10.1016/j.petrol.2011.12.024.

[20] M. Kané, M. Djabourov, J.L. Volle, Rheology and structure of waxy crude oils in quiescent and under shearing conditions, Fuel 83 (11–12) (2004) 1591–1605, https://doi.org/10.1016/j.fuel.2004.01.017.

[21] F.H. Marchesini, A.A. Alicke, P.R. De Souza Mendes, C.M. Ziglio, Rheological characterization of waxy crude oils: sample preparation, Energy Fuels. 26 (5) (2012) 2566–2577, https://doi.org/10.1021/ef201335c.

[22] X. Yin, H. Liu, C. Yang, Research status and prospect of rheology of waxy crude oil, Chem. Technol. Fuels Oils 60 (4) (2024) 954–969, https://doi.org/10.1007/s10553-024-01758-y.

[23] S. Zheng, M. Saidoun, T. Palermo, K. Mateen, H.S. Fogler, Wax deposition modeling with considerations of Non-Newtonian characteristics: application on field-scale pipeline, Energy Fuels. 31 (5) (2017) 5011–5023, https://doi.org/10.1021/acs.energyfuels.7b00504.

[24] L.F.R. Dalla, E.J. Soares, R.N. Siqueira, Start-up of waxy crude oils in pipelines, J Nonnewt. Fluid Mech 263 (2019) 61–68, https://doi.org/10.1016/j.jnnfm.2018.11.008.

[25] Fleming, F., Montesanti, J.R., Camargo, R., & Gonçalves, M. (2013). *OTC 24531 Lessons Learned on Wax Issues from Deep Offshore Brazil*.

[26] R. Mendes, G. Vinay, P. Coussot, Yield stress and minimum pressure for simulating the flow restart of a waxy crude oil pipeline, Energy Fuels. 31 (1) (2017) 395–407, https://doi.org/10.1021/acs.energyfuels.6b02576.

[27] K. Sarkodie, A.F. Rees, M. Abdulkadir, N.Y. Asiedu, J.A. Quaye, P. Boakye, Novel gas-liquid volumetric flow measurement via non-intrusive optical sensing under upward vertical bubbly flow, Exp. Comput. Multiph. Flow. 7 (4) (2025) 516–536, https://doi.org/10.1007/s42757-024-0230-1.

[28] M. Wu, J. Zhang, N. Gui, Q. Zou, X. Yang, J. Tu, S. Jiang, Z. Liu, Advances in the modeling of multiphase flows and their application in nuclear engineering—A review, Exp. Comput. Multiph. Flow. 6 (4) (2024) 287–352, https://doi.org/10.1007/s42757-024-0202-5.

[29] B.A. Tarcha, B.P. Bárbara, E.J. Soares, R.L. Thompson, Critical quantities on the yielding process of waxy crude oils, Rheol. Acta 54 (6) (2015) 479–499, https://doi.org/10.1007/s00397-015-0835-1.

[30] S.A. Ogunwale, K. Mateen, T. Palermo, A. Shetty, L. Mahir, A. Fidel-Dufour, R. G. Larson, Dependence of rheological behavior of waxy oils on wax composition and cooling and shear histories, J Rheol (N N Y) 69 (5) (2025) 713–730, https://doi.org/10.1122/8.0001006.

[31] A. Fakroun, H. Benkreira, Rheology of waxy crude oils in relation to restart of gelled pipelines, Chem. Eng. Sci. 211 (2020) 115212, https://doi.org/10.1016/j.ces.2019.115212.

[32] A. Japper-Jaafar, P.T. Bhaskoro, L.L. Sean, M.Z. Sariman, H. Nugroho, Yield stress measurement of gelled waxy crude oil: gap size requirement, J Nonnewt. Fluid Mech 218 (2015) 71–82, https://doi.org/10.1016/j.jnnfm.2015.02.001.

[33] R. Mendes, G. Vinay, G. Ovarlez, P. Coussot, Reversible and irreversible destructuring flow in waxy oils: an MRI study, J Nonnewt. Fluid Mech 220 (2015) 77–86, https://doi.org/10.1016/j.jnnfm.2014.09.011.

[34] L.T. Wardhaugh, D.V. Boger, The measurement and description of the yielding behavior of waxy crude oil, J Rheol (N N Y) 35 (6) (1991) 1121–1156, https://doi.org/10.1122/1.550168.

[35] H.A. Barnes, The 'yield stress myth?' Paper –21 years on, Appl. Rheol. 17 (4) (2007) 43110–1-43110-5, https://doi.org/10.1515/arh-2007-0012, 43110-1-43110–43115.

[36] Chang, C., Boger, D.V., & Dzuy Nguyen, Q. (1998). *The Yielding of Waxy Crude Oils*.

[37] R. Mendes, G. Vinay, G. Ovarlez, P. Coussot, Modeling the rheological behavior of waxy crude oils as a function of flow and temperature history, J Rheol (N N Y) 59 (3) (2015) 703–732, https://doi.org/10.1122/1.4916531.

[38] C.J. Dimitriou, G.H. McKinley, R. Venkatesan, Rheo-PIV analysis of the yielding and flow of model waxy crude oils, Energy Fuels. 25 (7) (2011) 3040–3052, https://doi.org/10.1021/ef2002348.

[39] T.O. Marinho, F.H. Marchesini, M.C.K. de Oliveira, M. Nele, Apparent wall slip effects on rheometric measurements of waxy gels, J Rheol (N N Y) 65 (2) (2021) 257–272, https://doi.org/10.1122/8.0000111.

[40] J. Huang, J. Zhang, W. Liu, Y. Xie, Q. Huang, H. Li, Universal correlation to reconcile yielding characterizations of waxy oil gels, Energy Fuels. 35 (5) (2021) 3798–3807, https://doi.org/10.1021/acs.energyfuels.0c03652.

[41] E.E.S. Ong, S. O'Byrne, J.L. Liow, Yield stress measurement of a thixotropic colloid, Rheol. Acta 58 (6–7) (2019) 383–401, https://doi.org/10.1007/s00397-019-01154-y.

[42] H. Liu, Y. Lu, J. Zhang, A comprehensive investigation of the viscoelasticity and time-dependent yielding transition of waxy crude oils, J Rheol (N N Y) 62 (2) (2018) 527–541, https://doi.org/10.1122/1.5002589.

[43] L.-P. Guo, J.-J. Zhang, L. Wang, R. Chen, B.-J. Liu, Mesoscopic mechanism of shear breakdown and static recovery characteristics of waxy crude oil gel structures, Pet. Sci. (2026), https://doi.org/10.1016/j.petsci.2026.01.035.

[44] B. Jia, J. Zhang, Yield behavior of waxy crude gel: effect of isothermal structure development before prior applied stress, Ind. Eng. Chem. Res. 51 (33) (2012) 10977–10982, https://doi.org/10.1021/ie301047g.

[45] Ekweribe, C., Civan, F., of Oklahoma, U., Su Lee, H., & Singh, P. (2009). *Interim Report on Pressure Effect on Waxy-Crude Pipeline-Restart Conditions Investigated by a Model System*.

[46] M.J. Martín-Alfonso, F.J. Martínez-Boza, F.J. Navarro, M.P. Fernandéz, C. Gallegos, Pressure-temperature-viscosity relationship for heavy petroleum fractions, Fuel 86 (1–2) (2007) 227–233, https://doi.org/10.1016/j.fuel.2006.05.006.

[47] M.J. Martín-Alfonso, F.J. Martínez-Boza, P. Partal, C. Gallegos, Influence of pressure and temperature on the flow behaviour of heavy fuel oils, Rheol. Acta 45 (4) (2006) 357–365, https://doi.org/10.1007/s00397-005-0051-5.

[48] F.J. Martínez-Boza, M.J. Martín-Alfonso, C. Gallegos, M.P. Fernandéz, High-pressure behavior of intermediate fuel oils, Energy Fuels. 25 (11) (2011) 5138–5144, https://doi.org/10.1021/ef200958v.

[49] L.C. Vieira, M.B. Buchuid, E.F. Lucas, Effect of pressure on the crystallization of crude oil waxes. I. selection of test conditions by microcalorimetry, Energy Fuels. 24 (4) (2010) 2208–2212, https://doi.org/10.1021/ef900711d.

[50] H. Li, J. Gong, The pressure effect on rheological behavior of water content of waxy crude oil, Pet. Sci. Technol. 29 (13) (2011) 1344–1352, https://doi.org/10.1080/10916460903502522.

[51] Y. Cheng, K.M. Brown, R.K. Prud'homme, Characterization and intermolecular interactions of hydroxypropyl guar solutions, Biomacromolecules. 3 (3) (2002) 456–461, https://doi.org/10.1021/bm0156227.
[52] S. Mortazavi-Manesh, J.M. Shaw, Effect of pressure on the rheological properties of Maya crude oil, Energy Fuels. 30 (2) (2016) 759–765, https://doi.org/10.1021/acs.energyfuels.5b02366.
[53] S. Sakthivel, S. Velusamy, Eco-efficient rheological improvement of heavy crude oil using lactam based ionic liquids at high temperature high pressure condition, Fuel 276 (2020) 118027, https://doi.org/10.1016/j.fuel.2020.118027.
[54] S. Sakthivel, S. Velusamy, Effect of ammonium based ionic liquids on the rheological behavior of the heavy crude oil for high pressure and high temperature conditions, Petroleum 8 (4) (2022) 552–566, https://doi.org/10.1016/J.PETLM.2021.06.002.
[55] H. Motahhari, M.A. Satyro, S.D. Taylor, H.W. Yarranton, Extension of the expanded fluid viscosity model to characterized oils, Energy Fuels. 27 (4) (2013) 1881–1898, https://doi.org/10.1021/ef301575n.
[56] P.V. Ramírez-González, S.E. Quiñones-Cisneros, Rheological behavior of heavy and extra-heavy crude oils at high pressure, Energy Fuels. 34 (2) (2020) 1268–1275, https://doi.org/10.1021/acs.energyfuels.9b02867.
[57] S. Velusamy, S. Sakthivel, J.S. Sangwai, Effects of imidazolium-based ionic liquids on the rheological behavior of heavy crude oil under high-pressure and high-temperature conditions, Energy Fuels. 31 (8) (2017) 8764–8775, https://doi.org/10.1021/acs.energyfuels.7b00521.
[58] A. Japper-Jaafar, P.T. Bhaskoro, Z.S. Mior, A new perspective on the measurements of wax appearance temperature: comparison between DSC, thermomicroscopy and rheometry and the cooling rate effects, J. Pet. Sci. Eng. 147 (2016) 672–681, https://doi.org/10.1016/j.petrol.2016.09.041.
[59] J. Chen, J. Zhang, H. Li, Determining the wax content of crude oils by using differential scanning calorimetry, Thermochim. Acta 410 (1–2) (2004) 23–26, https://doi.org/10.1016/S0040-6031(03)00367-8.
[60] Kok, M.V., L~toff&, J.-M., Claudy, P., Martin, D., Garcin, M., & Vollet, J.-L. (1996). *Comparison of wax appearance temperatures of crude oils by differential scanning calorimetry, thermomicroscopy and viscometry* (Vol. 75, Number 96).
[61] Henaut, I., Argillier, J.-F., & Pierre, C. (2003). *OTC 15278 Thermal Flow Properties of Heavy Oils*.
[62] C. Van Der Geest, V.C.B. Guersoni, A.C. Bannwart, Experimental study of the time to restart the flow of a gelled waxy crude in rheometer and pipeline, J. Pet. Sci. Eng. 181 (2019) 106247, https://doi.org/10.1016/j.petrol.2019.106247.
[63] A.K. Aboul-Gheit, T. Abd-el-Moghny, M.M. Al-Eseimi, Characterization of oils by differential scanning calorimetry, Thermochim. Acta 306 (1–2) (1997) 127–130, https://doi.org/10.1016/S0040-6031(97)00312-2.
[64] I. Hénaut, O. Vincké, F. Brucy, Waxy crude oil restart: mechanical properties of gelled oils, in: SPE Annual Technical Conference and Exhibition, 1999, https://doi.org/10.2118/56771-MS.
[65] H.S. Lee, P. Singh, W.H. Thomason, H.S. Fogler, Waxy oil gel breaking mechanisms: adhesive versus cohesive failure, Energy Fuels. 22 (1) (2008) 480–487, https://doi.org/10.1021/ef700212v.
[66] A.W. Sisko, The flow of lubricating greases, Ind. Eng. Chem. 50 (12) (1958) 1789–1792, https://doi.org/10.1021/ie50588a042.
[67] M.J. Martín-Alfonso, A. Mejía, F.J. Martínez-Boza, J.E. Martín-Alfonso, Rheological characterization of sepiolite-vegetable oil suspensions at high pressures, Appl. Clay. Sci. 212 (2021) 106220, https://doi.org/10.1016/j.clay.2021.106220.
[68] M.J. Martín-Alfonso, A. Mejía, F.J. Martínez-Boza, P. Partal, The influence of alkyl ammonium modifiers on the microstructure and high-pressure rheology of sepiolite-vegetable oil dispersions, Appl. Clay. Sci. 247 (2024) 107210, https://doi.org/10.1016/j.clay.2023.107210.
[69] J.J. Magda, H. El-Gendy, K. Oh, M.D. Deo, A. Montesi, R. Venkatesan, Time-dependent rheology of a model waxy crude oil with relevance to gelled pipeline restart, Energy Fuels. 23 (3) (2009) 1311–1315, https://doi.org/10.1021/ef800628g.
[70] G.T. Chala, S.A. Sulaiman, Voids size distribution in gelled waxy crude oil under dynamic and static cooling, Pet. Res. 9 (1) (2024) 109–114, https://doi.org/10.1016/j.ptlrs.2023.08.001.
[71] J.J.C. Hsu, M.M. Santamaria, J.P. Brubaker, P. Hawker, Wax deposition and gel strength of waxy live crudes, Offshore Technol. Conf. (1994), https://doi.org/10.4043/7573-MS.
[72] T.M. Williams, J.J.C. Hsu, H.L. Patterson, Measurement of break away yield stress of waxy crude oil and pipeline restart system design, in: Offshore Technology Conference, 1996, https://doi.org/10.4043/8231-MS.
[73] H. Zhu, Y. Lei, C. Li, B. Yao, F. Yang, S. Li, H. Peng, P. Yu, Experimental and mechanism investigation on flowability and wax deposition of waxy crude oil with dissolved CH4 by pressurized laboratory apparatus, Fuel 343 (2023) 127907, https://doi.org/10.1016/j.fuel.2023.127907.
[74] P.J. Hesse, R. Battino, P. Scharlin, E. Wilhelm, Solubility of gases in liquids. 20. Solubility of He, Ne, Ar, Kr, N2, O2, CH4, CF4, and SF6 in n-alkanes n-ClH2l+2 (6 $\leq$ l $\leq$ 16) at 298.15 K, J. Chem. Eng. Data 41 (2) (1996) 195–201, https://doi.org/10.1021/je9502455.
[75] L.C. Vieira, M.B. Buchuid, E.F. Lucas, Effect of pressure on the crystallization of crude oil waxes. II. evaluation of crude oils and condensate, Energy Fuels. 24 (4) (2010) 2213–2220, https://doi.org/10.1021/ef900761t.
[76] Q. Quan, W. Ran, L. Yang, G. Gao, S. Wang, J. Gong, The effect of pressure on wax deposition from wax-solvent mixtures with natural gas, J. Pet. Sci. Eng. 171 (2018) 1318–1325, https://doi.org/10.1016/j.petrol.2018.08.040.
[77] B.-F. Li, M.-P. Yang, G. Liu, L.-M. Zheng, C. Yang, Study on the effect of CH4 dissolution on the microstructure of wax crystal in waxy crude oil, Pet. Sci. 19 (4) (2022) 1853–1865, https://doi.org/10.1016/j.petsci.2022.04.007.
[78] A. Beerbower, D.F. Greene, The behavior of lubricating oils In inert gas atmospheres, S L Trans. 4 (1) (1961) 87–96, https://doi.org/10.1080/05698196108972422.
[79] I.F. Luthi, Waxy crude oil characterization and experimental study of the restart of a line blocked with gelled Waxy crude, in: SPE Annual Technical Conference and Exhibition, 2013, https://doi.org/10.2118/167625-STU.
[80] A.K. Doolittle, D.B. Doolittle, Studies in newtonian flow. V. Further verification of the free-space viscosity equation, J. Appl. Phys. 28 (8) (1957) 901–905, https://doi.org/10.1063/1.1722884.